Numerical scheme for evaluating the collision integrals for triple interactions in relativistic plasma

M. A. Prakapenia,[1, 2, a)] I. A. Siutsou,[3, b)] and G. V. Vereshchagin[4, 5, c)]

[1)]*ICRANet-Minsk, Institute of physics, National academy of sciences of Belarus, 220072 Nezaležnasci Av. 68-2, Minsk, Belarus*

[2)]*Department of Theoretical Physics and Astrophysics, Belarusian State University, 220030 Nezaležnasci Av. 4, Minsk, Belarus*

[3)]*Institute of Physics, Belarus National Academy of Sciences, Nezavisimosti Ave. 68, 220072 Minsk, Belarus*

[4)]*ICRANet, 65122 Piazza della Repubblica, 10, Pescara, Italy*

[5)]*INAF – Istituto di Astrofisica e Planetologia Spaziali, 00133 Via del Fosso del Cavaliere, 100, Rome, Italy*

(Dated: 1 March 2022)

Binary interactions in relativistic plasma, such as Coulomb and Compton scattering as well as pair creation and annihilation are well known and studied in details. Triple interactions, namely relativistic bremsstrahlung, double Compton scattering, radiative pair production, triple pair production/annihilation and their inverse processes, are usually considered as emission processes in astrophysical problems, as well as in laboratory plasmas. Their role in plasma kinetics is fundamental[1]. We present a new conservative scheme for computation of Uehling-Uhlenbeck collision integral for all triple interactions in relativistic plasma based on direct integration of exact QED matrix elements. Reaction rates for thermal distributions are compared, where possible, with the corresponding analytic expressions, showing good agreement. Our results are relevant for quantitative description of relativistic plasmas out of equilibrium, both in astrophysical and laboratory conditions.

I. INTRODUCTION

Electron-positron plasma is present in many astrophysical systems[2,3]. It is also studied in laboratory experiments with ultra-intense lasers and high energy beams[4]. Relativistic plasma has been the subject of extensive research since the 1970s. Many works focused on binary relaxation via Coulomb collisions between ions and electrons[5–10], with a special role of electron-positron creation and annihilation process[11,12]. Most papers consider an optically thin or mildly optically thick regime[11,13–15]. Equilibrium in the pair plasma has been studied in[11,14,15]. The energy loss rate by different processes has been analyzed in[16–18]. The conditions of dominance of the double Compton scattering versus bremsstrahlung were discussed in[19,20].

While the binary interactions between photons and electrons are the subject of classical textbooks in QED, the triple interactions such as electron-electron bremsstrahlung, double Compton scattering, three photon annihilation radiative pair production and their inverse are less represented in the literature. The theory of these processes is reviewed in[21–23]. The differential cross section and energy loss rate of electron-electron bremsstrahlung is studied in[24,25], and interaction rates are obtained for non-relativistic[26] and ultra-relativistic cases[27], respectively. The case of electron-positron bremsstrahlung is considered in[28]. The differential cross section for the radiative pair production is obtained in[29], while the total cross section is found in[30]. The three-photon anni-

hilation is studied in[31,32]. The theory of the double Compton scattering is developed in[33]. The cross-section for the non-relativistic case is obtained in[20,34], the emission rate in the soft photon limit is obtained in[35], while the rate at non-relativistic temperatures is derived in[36,37]. In summary, this vast literature presents analytic expressions for reaction rates in equilibrium. Non-equilibrium rates in relativistic regime can be computed only numerically.

Astrophysical observations indicate that out of equilibrium relativistic plasma is present in such sources as active galactic nuclei, binary X-ray sources, microquasars and gamma-ray bursts[3]. Energy release in the early Universe may bring primeval relativistic plasma out of equilibrium as well[38]. In laboratory conditions relativistic electron-positron jets are generated by interaction of intense laser pulses with condensed matter[39–41]. Hence most general description of relativistic plasma dynamics is required, which is given in terms of distribution function, where particle collisions are described by the integrals of differential cross-section (or a matrix element) over the phase space[42,43]. So far efficient codes were developed which describe only binary collisions without induced emission[44], binary collisions with induced emission[45], or binary and triple collisions not far from thermal equilibrium[46]. In this paper we generalize our method for calculation of collision integrals specifically treating triple interactions in relativistic plasma. In addition, the new kinematic approach, which improve the scheme performance, is presented for triple interactions.

This scheme was first introduced in the work[47] and then applied to the study of thermalization in relativistic plasma of Boltzmann particles[1,48–50], for the computation of relaxation timescales[51], and description of electron-positron plasma creation in strong electric fields[52]. Thermalization process was studied taking into account plasma degeneracy in[53]. In con-

[a)]Electronic mail: nikprokopenya@gmail.com
[b)]Electronic mail: i.siutsou@dragon.bas-net.by
[c)]Electronic mail: veresh@icra.it

<div style="text-align:center">TABLE I. Particle interactions in relativistic plasma</div>

Binary interactions	Triple interactions
Compton scattering	Double Compton scattering
$e^\pm \gamma \longrightarrow e^{\pm\prime}\gamma^\prime$	$e^\pm \gamma \longleftrightarrow e^{\pm\prime}\gamma^\prime\gamma^{\prime\prime}$
Coulomb, Møller and Bhabha scattering	Bremsstrahlung
$e_1^\pm e_2^\pm \longrightarrow e_1^{\pm\prime} e_2^{\pm\prime}$ $e^+ e^- \longrightarrow e^{+\prime} e^{-\prime}$	$e_1^\pm e_2^\pm \longleftrightarrow e_1^{\pm\prime} e_2^{\pm\prime}\gamma$ $e^+ e^- \longleftrightarrow e^{+\prime} e^{-\prime}\gamma$
Pair production/annihilation	Three-photon pair production/annihilation
$e^+ e^- \longleftrightarrow \gamma_1 \gamma_2$	$e^+ e^- \longleftrightarrow \gamma_1 \gamma_2 \gamma_3$
	Radiative pair production/annihilation
	$\gamma_1 \gamma_2 \longleftrightarrow e^+ e^- \gamma$ $e^\pm \gamma \longleftrightarrow e^{\pm\prime} e^+ e^-$

trast with non-degenerate plasma described by Boltzmann equations, quantum statistics is taken into account by adopting the Uehling-Uhlenbeck equation, which contains additional Pauli blocking and Bose enhancement multipliers[54,55]. It was shown that effects of plasma degeneracy lead to interesting new phenomena such as Bose condensation of photons[56], and avalanche thermalization due to Pauli blocking[57].

This paper is structured as follows. In Section 2 the relativistic Boltzmann equation with collision integrals for relativistic plasma is introduced. In Section 3 numerical treatment for calculation of collision integrals for all binary and triple interactions in relativistic plasma is described. In Section 4 numerical results are reported, and compared and contrasted with existing results in the literature. In Section 5 main results are summarized.

II. RELATIVISTIC BOLTZMANN EQUATION AND COLLISION INTEGRALS

In a homogeneous and isotropic electron-positron plasma kinetic equations for distribution functions f are[3]:

$$\frac{d}{dt} f(\mathbf{p},t) = \sum_q (\eta^q - \chi^q f(\mathbf{p},t)), \qquad (1)$$

where the summation index q denotes all processes of interaction between plasma particles, η^q and χ^q are emission and absorption coefficients correspondingly, $\mathbf{p}$ is particle three-momentum, t is time. The distribution function is normalized such that the number density is given by $n = \int f(\mathbf{p}) \, d^3p$. We take into account all binary and triple interactions listed in Table I. The treatment of binary interactions is covered by many textbooks on relativistic kinetic theory, see e.g.[42,43]. Instead, triple interactions are not considered. Accounting for such interactions is essential for understanding radiation from plasma, but also for understanding of thermalization process[1,3].

Consider a triple interaction: two incoming particles of kinds I and II in quantum states 1 and 2 produce three outgoing particles of kinds III, IV, and V in quantum states 3, 4, and 5. Let momenta of particles before interaction be $\mathbf{p_1}$ and

$\mathbf{p}_2$, and after interaction be $\mathbf{p}_3$, $\mathbf{p}_4$, and $\mathbf{p}_5$, correspondingly. This process can be represented symbolically as

$$I_1 + II_2 \longrightarrow III_3 + IV_4 + V_5. \qquad (2)$$

The inverse process is

$$III_3 + IV_4 + V_5 \longrightarrow I_1 + II_2. \qquad (3)$$

Energy ε and momentum conservation gives

$$\varepsilon_1 + \varepsilon_2 = \varepsilon_3 + \varepsilon_4 + \varepsilon_5, \qquad \mathbf{p}_1 + \mathbf{p}_2 = \mathbf{p}_3 + \mathbf{p}_4 + \mathbf{p}_5. \qquad (4)$$

In the Uehling-Uhlenbeck equation collision integrals for particle I in the state 1 is a function of momentum $\mathbf{p}_1$[58] and time[54,55]

$$\eta_I(\mathbf{p}_1,t) - \chi_I(\mathbf{p}_1,t) f_I(\mathbf{p}_1,t) = \int d^3\mathbf{p}_2 d^3\mathbf{p}_3 d^3\mathbf{p}_4 d^3\mathbf{p}_5$$
$$\times \left[W_{(3,4,5|1,2)} f_{III} f_{IV} f_V \times \left(1 \pm \bar{f}_I\right)\left(1 \pm \bar{f}_{II}\right) \right.$$
$$\left. - W_{(1,2|3,4,5)} f_I f_{II} \times \left(1 \pm \bar{f}_{III}\right)\left(1 \pm \bar{f}_{IV}\right)\left(1 \pm \bar{f}_V\right) \right], \quad (5)$$

where $\bar{f}_I = h^3 f_I(\mathbf{p}_1,t)/g_I$ and so on, g being the number of degenerate spin states (for our plasma it is 2 for all components), h is Planck's constant, and W are the transition functions. The first term in the square brackets corresponds to emission of particle I in the inverse process (3), while the second term corresponds to absorption of particle I in the direct process (2). This is the general case when all the kinds of incoming and outgoing particles are different.

It is also possible that particles before and after the interaction are of the same kind. In this case collision integrals become more involved. Without loss of generality consider the case when $I = V$. Then two new terms appear in the collision integral of particle I of state 1: emission coefficient $\eta_I(\mathbf{p}_1,t)$ in the direct process $I_5 + II_2 \longrightarrow III_3 + IV_4 + I_1$, and absorption coefficient $\chi_I(\mathbf{p}_1,t) f_I(\mathbf{p}_1,t)$ in the inverse process $III_3 + IV_4 + I_1 \longrightarrow I_5 + II_2$. Combining all these terms we obtain the collision integral

$$\eta_I(\mathbf{p}_1,t) - \chi_I(\mathbf{p}_1,t) f_I(\mathbf{p}_1,t) = \int d^3\mathbf{p}_2 d^3\mathbf{p}_3 d^3\mathbf{p}_4 d^3\mathbf{p}_5$$
$$\times \left[-W_{(1,2|3,4,5)} f_I f_{II} \times \left(1 \pm \bar{f}_{III}\right)\left(1 \pm \bar{f}_{IV}\right)\left(1 \pm \bar{f}_V\right) \right.$$
$$+ W_{(3,4,5|1,2)} f_{III} f_{IV} f_V \times \left(1 \pm \bar{f}_I\right)\left(1 \pm \bar{f}_{II}\right)$$
$$+ W_{(5,2|3,4,1)} f_V f_{II} \times \left(1 \pm \bar{f}_{III}\right)\left(1 \pm \bar{f}_{IV}\right)\left(1 \pm \bar{f}_I\right)$$
$$\left. - W_{(3,4,1|5,2)} f_{III}(\mathbf{p}_3,t) f_{IV}(\mathbf{p}_4,t) f_I(\mathbf{p}_1,t) \times \left(1 \pm \bar{f}_V\right)\left(1 \pm \bar{f}_{II}\right) \right].$$
$$(6)$$

All triple QED-processes listed in Table I, with the only exception of three-photon pair production/annihilation, are represented by four-term collision integrals. These four terms in particular case of double Compton scattering with corresponding quantum symmetrization multipliers were for the

first time discussed by Chluba[59]. In previous works this fact was ignored and only two terms were considered in collision integrals, see e.g.[19,37]. It should be noted that some properties of plasma, e.g. the detailed balance conditions, may be studied based on only two terms in collision integrals. However, the structure of all four coefficients is different, and their presence in collision integral (6) is essential.

In direct triple interactions transition function W can be expressed through differential cross-section $d\sigma$. Using the definition of $d\sigma$[60] (Eq. (64.18)) and its relation to number of interactions $dN/dV\,dt$ per unit volume per unit time from equation (12.7) of[61], we arrive to

$$W_{(1,2|3,4,5)}d^3\mathbf{p}_3 d^3\mathbf{p}_4 d^3\mathbf{p}_5$$
$$= c\frac{\sqrt{[\varepsilon_1\varepsilon_2-(\mathbf{p}_1\cdot\mathbf{p}_2)c^2]^2-(m_I m_{II}c^4)^2}}{\varepsilon_1\varepsilon_2}d\sigma. \quad (7)$$

The differential cross-section in turn is related to the QED matrix element squared, averaged over incoming particle polarizations and summed over outgoing particle polarizations X, see[62] (Eq. (11.31)). Therefore

$$W_{(1,2|3,4,5)} = \frac{\alpha r_e^2}{(4\pi)^2}\frac{c^7 X}{\varepsilon_1\varepsilon_2\varepsilon_3\varepsilon_4\varepsilon_5}$$
$$\times \delta(\varepsilon_{initial}-\varepsilon_{final})\delta^3(\mathbf{p}_{initial}-\mathbf{p}_{final}), \quad (8)$$

where $r_e = e^2/m_e c^2$ is the classical electron radius and α is the fine structure constant. For double Compton scattering X is given by equations (3), (9), (10) of[33]. For relativistic bremsstrahlung $X = 16A$, where A is given in Appendix B of[63].

For all other triple processes listed in Table I the matrix elements can be obtained from two aforementioned ones applying the substitution rule, see e.g.[62] (Sec. 8.5). For example, exchanging incoming photon with outgoing electron or positron in double Compton scattering

$$e_1^- + \gamma_2 \longrightarrow e_3^- + \gamma_4 + \gamma_5$$

the three-photon pair creation-annihilation

$$e_1^- + e_3^+ \longrightarrow \gamma_2 + \gamma_4 + \gamma_5$$

process is recovered. Then the matrix element X of this process can be derived from X of the one of the double Compton scattering by the following substitutions

$$\mathbf{p}_3 \longrightarrow -\mathbf{p}_3, \quad \varepsilon_3 \longrightarrow -\varepsilon_3, \quad \mathbf{p}_2 \longrightarrow -\mathbf{p}_2, \quad \varepsilon_2 \longrightarrow -\varepsilon_2. \quad (9)$$

In order to get collision integrals for inverse triple interactions we can make use of detailed equilibrium conditions, valid for QED interactions[43,64], that gives

$$\frac{h^3}{g_{III}}\frac{h^3}{g_{IV}}\frac{h^3}{g_V}W_{(1,2|3,4,5)} = \frac{h^3}{g_I}\frac{h^3}{g_{II}}W_{(3,4,5|1,2)}, \quad (10)$$

and since in our case all $g = 2$ we finally obtain

$$h^3 W_{(1,2|3,4,5)} = 2W_{(3,4,5|1,2)}, \quad (11)$$

The collision rate is a multidimensional integral over the phase space of interacting particles, which spans $4 \times 3 = 12$ dimensions for binary interactions and $5 \times 3 = 15$ dimensions for triple ones. The energy-momentum conservation allows to perform integration over 4 variables, while spherical symmetry in the phase space allows to perform additional three integrals, leaving 5 and 8 integrals for binary and triple interactions, correspondingly. From the computational viewpoint this problem is highly demanding. In the next section we introduce the fast numerical scheme dealing with it.

III. NUMERICAL TREATMENT OF THE COLLISION INTEGRALS

The main difference between the approach to the kinetics of plasma with Boltzmann equations[1,49,51] and the present approach with Uehling-Uhlenbeck equations appears in the dependence of emission and absorption coefficients not only on the distributions of the incoming particles, but the on distributions of the outgoing particles as well, owing to the presence of Bose enhancement and Pauli blocking factors (further referred to as quantum corrections). Due to this difference in what follows we adopt a "process-oriented" technique[45,53].

Due to the spherical symmetry in the phase space[65], we introduce spherical coordinates and discretize it. Zone $\Omega_{a,j,k}^I$ of particle kind I corresponds to energy ε_a, cosine of polar angle μ_j and azimuthal angle ϕ_k, where indices span the ranges $1 \le a \le n_\varepsilon$, $1 \le j \le n_\mu$, $1 \le k \le n_\phi$. Zone edges are $\varepsilon_{a\mp1/2}$, $\mu_{j\mp1/2}$, $\phi_{k\mp1/2}$. Width of a-th energy zone Ω_a^I is equal to $\Delta\varepsilon_a \equiv \varepsilon_{a+1/2} - \varepsilon_{a-1/2}$. Due to isotropy f_I does not depend on μ and ϕ, therefore particle density I in the zone a is

$$Y_a^I(t) = 4\pi \int_{\varepsilon_{a-1/2}}^{\varepsilon_{a+1/2}} c^{-3}\varepsilon\sqrt{\varepsilon^2 - m_I^2 c^4}f_I(\varepsilon,t)d\varepsilon$$
$$\approx 4\pi c^{-3}\varepsilon_a\sqrt{\varepsilon_a^2 - m_I^2 c^4}f_I(\varepsilon_a,t)\Delta\varepsilon_a. \quad (12)$$

In these variables discretized Uehling-Uhlenbeck equation for particle I and energy zone a is

$$\frac{dY_a^I(t)}{dt} = \sum \left[\eta_a^I(t) - \chi_a^I(t)Y_a^I(t)\right], \quad (13)$$

where the sum is taken over all processes that include particle I. Emission and absorption coefficients on grid are obtained by integration of collision integrals over the zones, and these integrals are replaced by sums over the grid.

The exact conservation laws (particle number, energy, charge) are satisfied in the code thanks to implementation of the interpolation procedure for outgoing particles. The system under consideration has several characteristic timescales for different processes, and the resulting system of ordinary differential equations (13) is stiff. We use Gear's method[66] to integrate the system numerically.

A. Binary interactions

First we recall the treatment of binary interactions introduced in[45]. Spherical symmetry allows to perform three integrals over the angles of the first incoming particle and over the azimuthal angle of the second one: $\int d\mu_I d\phi_I d\phi_{II} \longrightarrow 8\pi^2$. P-symmetry of QED allows to reduce azimuthal angle range for the third particle $\int_0^{2\pi} d\phi_{III} \longrightarrow 2\int_0^\pi d\phi_{III}$. In addition, energy-momentum conservation expressed with the δ-function in the transition function (7) allows to perform additional four integrations, with the usual choice to exclude energy and angles of the first outgoing particle and energy of the second outgoing particle

$$\delta(\varepsilon_1 + \varepsilon_2 - \varepsilon_3 - \varepsilon_4)\delta^3(\mathbf{p}_1 + \mathbf{p}_2 - \mathbf{p}_3 - \mathbf{p}_4) =$$
$$c^2 \frac{\delta(\varepsilon_4 - \varepsilon_4^*)\delta(\varepsilon_3 - \varepsilon_3^*)\delta(\varphi_3 - \varphi_3^*)\delta(\mu_3 - \mu_3^*)}{\varepsilon_3 p_3 [1 - (\beta_3/\beta_4)\mathbf{n}_3 \cdot \mathbf{n}_4]}, \quad (14)$$

where $\beta = pc/\varepsilon$, asterisks denote values defined for excluded integration variables by the energy and momentum conservation

$$p_4^* = \frac{AB \pm \sqrt{A^2 + 4m_{IV}^2 c^2(B^2 - 1)}}{2(B^2 - 1)}, \quad (15)$$

$$A = \frac{c}{\varepsilon}\left[p^2 + (m_{III}^2 - m_{IV}^2)c^2\right] - \frac{\varepsilon}{c}, \qquad B = \frac{c}{\varepsilon}\mathbf{n}_4 \cdot \mathbf{p},$$

$$\varepsilon_4^* = c\sqrt{(p_4^*)^2 + m_{IV}^2 c^2}, \qquad \varepsilon_3^* = \varepsilon - \varepsilon_4^*, \qquad \mathbf{p}_3^* = \mathbf{p} - \mathbf{p}_4^*,$$

$$\mathbf{n}_i = \mathbf{p}_i/p_i, \quad \varepsilon = \varepsilon_1 + \varepsilon_2, \quad \mathbf{p} = \mathbf{p}_1 + \mathbf{p}_2.$$

Then the absorption coefficient for incoming particle I in binary interaction $I + II \to III + IV$ can be written as

$$\chi_a^I(t)Y_a^I(t) \approx \frac{\hbar^2 c^4}{8(4\pi)^2}\sum \Delta\mu_{II}\Delta\mu_{IV}\Delta\phi_{IV} \times |M_{fi}|^2$$

$$\times \frac{p_4}{\varepsilon_3[1 - (\beta_3/\beta_4)\mathbf{n}_3 \cdot \mathbf{n}_4]} \times \frac{Y_a^I(t)}{\varepsilon_a}\frac{Y_b^{II}(t)}{\varepsilon_b}$$

$$\times \left[1 \pm \frac{Y_{c'}^{III}(t)}{\bar{Y}_{c'}^{III}}\right]\left[1 \pm \frac{Y_{d'}^{IV}(t)}{\bar{Y}_{d'}^{IV}}\right], \quad (16)$$

where $\bar{Y}_a^I$ are defined as in eq. (12) with the substitution $f \to 2/h^3$ and index primes meaning is as follows.

The energies of incoming particles are fixed in the nodes of the grid, but the energies of outgoing particles are off the grid. In order to satisfy conservation laws (particle number, energy, charge) an interpolation procedure is implemented for outgoing particles. Each outgoing particle is split in two interpolated particles between the adjacent zones with a weight determined by its energy and the zone width[67]. Interpolation redistributes outgoing particle I of energy ε_a into two energy zones $\Omega_n^I, \Omega_{n+1}^I$ defined by $\varepsilon_n < \varepsilon_a < \varepsilon_{n+1}$, see Eq. (19) below.

Interpolation procedure for outgoing particles should satisfy the laws of quantum statistics. Any process where a fermion end up in a fully occupied zone is not allowed. We introduce therefore Bose enhancement and Pauli blocking coefficients as

$$\left[1 \pm \frac{Y_{a'}^I(t)}{\bar{Y}_{a'}^I}\right] = \min\left(1 \pm \frac{Y_n^I(t)}{\bar{Y}_n^I}, 1 \pm \frac{Y_{n+1}^I(t)}{\bar{Y}_{n+1}^I}\right). \quad (17)$$

This procedure allows us to fulfil quantum statistics requirements by the cost of partly reducing grid resolution.

Hence emission coefficient for outgoing particle I in inverse process is

$$\eta_a^I(t) \approx \frac{\hbar^2 c^4}{8(4\pi)^2}\sum C_a(\varepsilon_1)\Delta\mu_{IV}\Delta\mu_{II}\Delta\phi_{II} \times |M_{fi}|^2$$

$$\times \frac{p_2}{\varepsilon_1[1 - (\beta_1/\beta_2)\mathbf{n}_1 \cdot \mathbf{n}_2]} \times \frac{Y_c^{III}(t)}{\varepsilon_c}\frac{Y_d^{IV}(t)}{\varepsilon_d}$$

$$\times \left[1 \pm \frac{Y_{a'}^I(t)}{\bar{Y}_{a'}^I}\right]\left[1 \pm \frac{Y_{b'}^{II}(t)}{\bar{Y}_{b'}^{II}}\right], \quad (18)$$

where interpolation coefficients are

$$C_a(\varepsilon_1) = \begin{cases} \dfrac{\varepsilon_a - \varepsilon_1}{\varepsilon_a - \varepsilon_{a-1}}, & \varepsilon_{a-1} < \varepsilon_1 < \varepsilon_a, \\[2mm] \dfrac{\varepsilon_{a+1} - \varepsilon_1}{\varepsilon_{a+1} - \varepsilon_a}, & \varepsilon_a < \varepsilon_1 < \varepsilon_{a+1}, \\[2mm] 0, & \text{other } \varepsilon_1. \end{cases} \quad (19)$$

Integration over the angles can be made only once at the beginning of calculations[3,49], and we refer to this phase as integral coefficients calculation. Then we store corresponding integral coefficients for each set of incoming and outgoing particles in the form of three numbers $K_{1,2,3}$ giving for elementary terms in binary interaction $I + II \to III + IV$ the following contributions

$$\dot{Y}_a(t) = \dot{Y}_b(t) = -K_1^{abcd}D,$$
$$\dot{Y}_c(t) = K_2^{abcd}D, \quad \dot{Y}_{c+1}(t) = (K_1^{abcd} - K_2^{abcd})D,$$
$$\dot{Y}_d(t) = K_3^{abcd}D, \quad \dot{Y}_{d+1}(t) = (K_1^{abcd} - K_3^{abcd})D, \quad (20)$$
$$D = Y_a(t)Y_b(t)\left[1 \pm \frac{Y_{c'}(t)}{\bar{Y}_{c'}}\right]\left[1 \pm \frac{Y_{d'}(t)}{\bar{Y}_{d'}}\right],$$

that fulfil conservation laws by construction. Sum of all contributions from different elementary reactions gives total collision integrals on the grid with 2-nd order accuracy. As each stored elementary reaction gives 6 terms for the rates $\dot{Y}$ and we span elementary reaction space, and not $\dot{Y}$ themselves, we denote such an approach as "process-oriented". Looping through $\dot{Y}$ is a more traditional approach[49], but it demands 6-time separate treatment of the same D that slows down the calculations.

B. Triple interactions

The scheme is straightforwardly generalized to triple interactions. However, in contrast to the binary case where index

pairs I,II and III,IV can be swapped without any change in the structure of elementary terms (20), in triple case such a symmetry is absent. So emission and absorption coefficients for the processes (2) and (3) are discussed separately below. Further, standard choice of excluded δ-function integrations is not very convenient in this case as it leads to substantial slowdown of calculations due to the branching of solutions in algebraic equations (15) which requires execution of logical commands.
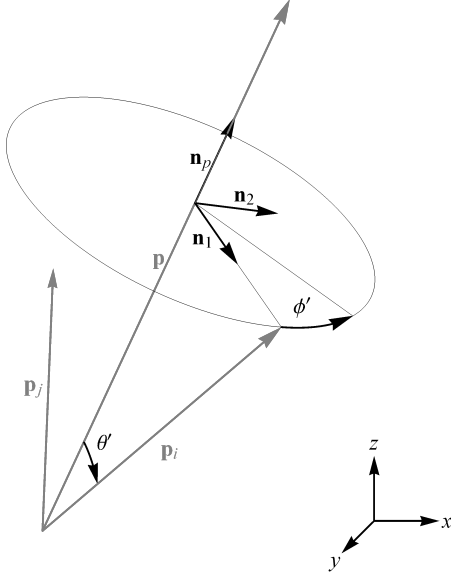

FIG. 1. The new coordinates adopted for numerical integration on the phase space.

In order to avoid this branching it is possible to use the variables of outgoing particle pair: a) the energy of one of these particles ε_i, b) its angle ϕ_i' defined as rotation angle of its momentum $\mathbf{p}_i$ around the direction of total pair momentum $\mathbf{p} = \mathbf{p}_i + \mathbf{p}_j$. This azimuthal angle ϕ_i' serves as an angle of auxiliary spherical coordinate system (μ', ϕ') with z' axis aligned with $\mathbf{p}$, see Fig. 1, so that the solution of energy and momentum conservation equations is unique

$$\varepsilon_j = \varepsilon - \varepsilon_i, \quad \phi_j' = \pi + \phi_i', \qquad (21)$$

$$\mu_i' = \frac{p^2 + p_i^2 - p_j^2}{2pp_i}, \quad \mu_j' = \frac{p^2 + p_j^2 - p_i^2}{2pp_j},$$

$$\mathbf{p}_i = p_i\left(\mu_i'\mathbf{n}_p + \sqrt{1-\mu_i'^2}\left[\mathbf{n}_1\cos\phi_i' + \mathbf{n}_2\sin\phi_i'\right]\right),$$

$$\mathbf{p}_j = p_j\left(\mu_j'\mathbf{n}_p + \sqrt{1-\mu_j'^2}\left[\mathbf{n}_1\cos\phi_j' + \mathbf{n}_2\sin\phi_j'\right]\right),$$

$$\mathbf{n}_p = \mathbf{p}/p, \quad p = \sqrt{\mathbf{p}\cdot\mathbf{p}}, \quad \varepsilon = \varepsilon_i + \varepsilon_j,$$

$$p_i = \sqrt{\varepsilon_i^2/c^2 - m_i^2 c^2}, \quad p_j = \sqrt{\varepsilon_j^2/c^2 - m_j^2 c^2},$$

where $\mathbf{n}_1$ and $\mathbf{n}_2$ are two orthogonal unit normals to $\mathbf{p}$. The

limits of integration are very simple

$$\phi_i' \in [0, 2\pi), \qquad \varepsilon_i \in [A-B, A+B], \qquad (22)$$

$$A = \frac{\varepsilon\left(\varepsilon^2 - p^2c^2 - m_j^2c^4 + m_i^2c^4\right)}{2\left(\varepsilon^2 - p^2c^2\right)},$$

$$B = \frac{pc\sqrt{\left(\varepsilon^2 - p^2c^2 - m_j^2c^4 - m_i^2c^4\right)^2 - (2m_im_jc^4)^2}}{2\left(\varepsilon^2 - p^2c^2\right)},$$

and δ-function becomes

$$\delta(\varepsilon - \varepsilon_i - \varepsilon_j)\delta^3(\mathbf{p} - \mathbf{p}_i - \mathbf{p}_j) = \frac{\delta(\mu_i - \mu_i^*)\delta(\varepsilon_j - \varepsilon_j^*)\delta(\mu_j' - \mu_j'^*)\delta(\phi_j' - \phi_j'^*)}{pp_ip_j}, \qquad (23)$$

where asterisks denote solution of kinematic equations (21).

The Jacobian (23) exhibits kinematic singularity with a clear physical origin: it appears when total or any particle momentum is zero. Singularities at $p_i = 0$ and $p_j = 0$ disappear at the collision integral as the corresponding rates tend to a constant due to velocity dependence. The only survived singularity is of zero total momentum $p = 0$: this turns out to be center-of-mass frame for the chosen particles and in this case the interval of ε_i in (22) reduces to a point $\varepsilon_i = A$, while μ_i' and ϕ_i' span all the sphere. As a result, this singularity in the integrand is compensated by shrinking of the integration limits of ε_i and the integral remains finite at this point. However, the subspace of $p = 0$ is of much lower dimension than the total phase space of integration (it is 3-dimensional one versus 6-dimensional one in our case), so this singularity problem can be avoided numerically just by rotating slightly each of the $\{\mu, \phi\}$ grids for the particles in the reaction to exclude calculations at the $p = 0$ points.

Additional advantage of this scheme is the ease of treatment of phase space symmetries: to exclude the same particle states from incomes and/or outcomes it is sufficient to use ascending (or descending) energy requirements for the same particles, i.e. in three-photon annihilation we just integrate only over $\varepsilon_{\gamma_1} < \varepsilon_{\gamma_2} < \varepsilon_{\gamma_3}$. In the traditional approach ε_{γ_2} and ε_{γ_3} are involved functions of angles of integration, that leads to another branching in the innermost integration calculations, or alternatively to calculation over all the phase space for photons (effectively increasing the amount of calculations 6-fold) and introduction of 1/6 multipliers after.

Finally, for the direct process (2) we arrive to the grid representation of the absorption coefficient for particle I in the following simple form

$$\chi_a^I(t)Y_a^I(t) \approx \frac{\alpha c r_e^2}{32\pi^2}\sum \Delta\mu_{II}\Delta\varepsilon_{III}\Delta\mu_{III}\Delta\phi_{III}\Delta\varepsilon_{IV}\Delta\phi_{IV}'$$

$$\times \frac{p_{III}}{p}X\frac{Y_a^I(t)}{\varepsilon_a}\frac{Y_b^{II}(t)}{\varepsilon_b}$$

$$\times \left[1\pm\frac{Y_{c'}^{III}(t)}{\bar{Y}_{c'}^{III}}\right]\left[1\pm\frac{Y_{d'}^{IV}(t)}{\bar{Y}_{d'}^{IV}}\right]\left[1\pm\frac{Y_{f'}^V(t)}{\bar{Y}_{f'}^V}\right], \qquad (24)$$

while for the emission coefficient of particle IV we have

$$
\eta_d^{IV}(t) \approx \frac{\alpha c r_e^2}{32\pi^2} \sum \Delta\mu_{II}\Delta\varepsilon_{III}\Delta\mu_{III}\Delta\phi_{III}\Delta\varepsilon_{IV}\Delta\phi'_{IV}
$$
$$
\times \frac{p_{III}}{p} X C_d(\varepsilon_{IV}) \frac{Y_a^I(t)}{\varepsilon_a} \frac{Y_b^{II}(t)}{\varepsilon_b}
$$
$$
\times \left[1 \pm \frac{Y_{c'}^{III}(t)}{\bar{Y}_{c'}^{III}}\right]\left[1 \pm \frac{Y_{d'}^{IV}(t)}{\bar{Y}_{d'}^{IV}}\right]\left[1 \pm \frac{Y_{f'}^{V}(t)}{\bar{Y}_{f'}^{V}}\right], \quad (25)
$$

the interpolation coefficient $C(\varepsilon)$ being defined in eq. (19) and primed indices having the meaning described after eq. (16). We use also special refined grid for ε_{IV}, that ensures the given number of integration points for each possible zone set of IV and V particles (typically 2 points, further refinement does not change results substantially). Analogous relations hold for the inverse process.

For each process the sum over the angles again can be performed only once, at the beginning of calculations. Elementary reaction now is represented by three numbers $K_{1,2,3}$ giving the following collision integral terms

$$
\dot{Y}_a(t) = \dot{Y}_b(t) = -\dot{Y}_c(t) = -K_1^{abcdf}D,
$$
$$
\dot{Y}_d(t) = K_2^{abcdf}D, \quad \dot{Y}_{d+1}(t) = (K_1^{abcdf} - K_2^{abcdf})D,
$$
$$
\dot{Y}_f(t) = K_3^{abcdf}D, \quad \dot{Y}_{f+1}(t) = (K_1^{abcdf} - K_3^{abcdf})D, \quad (26)
$$
$$
D = Y_a(t)Y_b(t)\left[1 \pm \frac{Y_{c'}(t)}{\bar{Y}_{c'}}\right]\left[1 \pm \frac{Y_{d'}(t)}{\bar{Y}_{d'}}\right]\left[1 \pm \frac{Y_{f'}(t)}{\bar{Y}_{f'}}\right],
$$

for direct reaction and

$$
\dot{Y}_a(t) = \dot{Y}_b(t) = \dot{Y}_c(t) = -K_1^{abcdf}D,
$$
$$
\dot{Y}_d(t) = K_2^{abcdf}D, \quad \dot{Y}_{d+1}(t) = (K_1^{abcdf} - K_2^{abcdf})D,
$$
$$
\dot{Y}_f(t) = K_3^{abcdf}D, \quad \dot{Y}_{f+1}(t) = (K_1^{abcdf} - K_3^{abcdf})D, \quad (27)
$$
$$
D = Y_a(t)Y_b(t)Y_c(t)\left[1 \pm \frac{Y_{d'}(t)}{\bar{Y}_{d'}}\right]\left[1 \pm \frac{Y_{f'}(t)}{\bar{Y}_{f'}}\right],
$$

for inverse reaction. To find rates $\dot{Y}$ we span elementary reaction space as in the case of binary interactions.

IV. NUMERICAL RESULTS

In this section the results of numerical calculations are presented. We compare our results for collision integral with all known analytical expressions in the literature. They appear to use only Boltzmann statistics

$$
\bar{f}_{eq} = \exp\left(-\frac{\varepsilon - \mu}{k_B T}\right), \quad (28)
$$

without quantum corrections, so in what follows all comparisons are done with such a case. Svensson[68] gives analytical expressions for thermal photon emission coefficients η_γ in the soft photon limit ($\varepsilon_\gamma \ll k_B T$) for the double Compton scattering, electron-electron bremsstrahlung, three-photon annihilation and radiative pair production. These rates are inversely proportional to the photon energy $\eta_\gamma \sim \varepsilon^{-1}$. We note
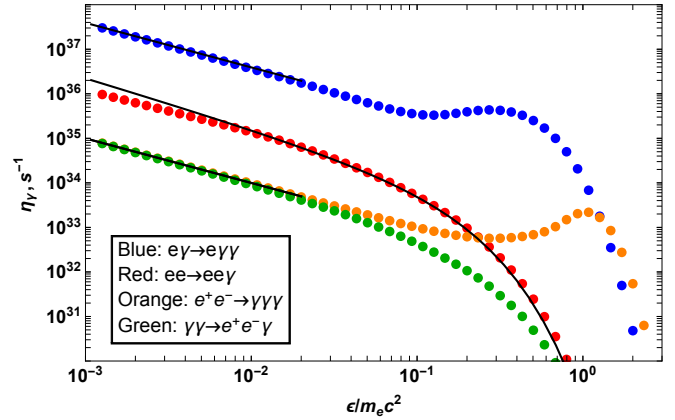

FIG. 2. Thermal photon emissivity η_γ as a function of photon energy. Solid curves represent Svensson[68] and Haug[24] analytical formulas, see text for details. From top to bottom: double Compton scattering, relativistic bremsstrahlung, three-photon annihilation, radiative pair production. The number of nodes is: 60 for energy, 32 for ϕ angle and 16 for μ angle. The distribution functions are taken at equilibrium with $\theta = 0.1$ and chemical potential being zero.

TABLE II. Numerical accuracy measured by the Q coefficient for selected number of angular grid nodes ($n_\varepsilon = 60, n_\phi = 2n_\mu$) for different interactions.

Process/n_μ	4	8	16	32
Double Compton scattering	0.143	0.087	0.044	0.049
relativistic bremsstrahlung	0.396	0.336	0.271	0.228
three photon annihilation	0.043	0.012	0.023	0.021
radiative pair production	0.275	0.133	0.085	0.075

that Svensson formula for electron-electron bremsstrahlung does not correctly describe the non-relativistic limit, therefore we use the formula of Haug[25], which represents non-relativistic limit. One should keep in mind that Svensson formulas represent an interpolation between non-relativistic and ultra-relativistic limits and their accuracy for the intermediate plasma temperatures is not estimated. For this reason we compare our results only in a non-relativistic domain, selecting for $k_B T = 0.1 m_e c^2$. Below dimensionless energy $e \equiv \varepsilon/m_e c^2$ and temperature $\theta = k_B T/m_e c^2$ are used.

The calculations are performed on a logarithmic energy grid with $n_\varepsilon = 60$ nodes, with different homogeneous grids for angular variables, ϕ-grid is 2 time denser then μ-grid (typically μ-grid contains $n_\mu = 16$ nodes). In order to resolve better soft photons we choose the lower particle energy boundary $0.001 m_e c^2$ and upper particle energy boundary $10 m_e c^2$. This energy region perfectly covers thermal distribution of particles from $\theta = 0.1$ to $\theta = 1$.

Figure 2 shows numerical thermal photon emissivity coefficient compared with analytic formulas (black curves). All solid curves besides bremsstrahlung are plotted up to the photon energy $e = 0.02$, as they are valid only in the soft photon limit. There is a good agreement with Svensson formula (A10) in[68] for the double Compton scattering (blue dots), see
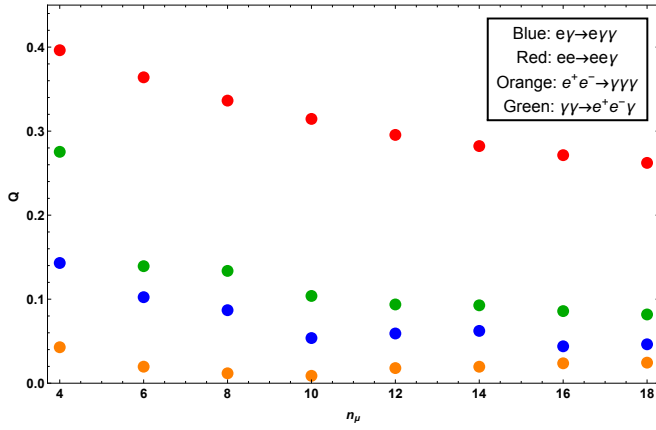
FIG. 3. Dependence of Q parameter defined in eq. (29) which characterize accuracy of the calculation of triple interactions on the number of nodes in angle variables. The accuracy increases with increasing number of nodes.

also Table II and Figure 3. Bremsstrahlung emissivity (red dots) show deviations from Haug formula (2.10) in[24] for soft photons; this deviation decreases with increasing resolution in angles, see Table II. Emissivities for three-photon annihilation (orange dots) and radiative pair production (green dots) are compared with eq. (A18) and (A20) in[68], respectively, differ by a factor of particle density in the case of non-zero chemical potential and become identical in the case of zero chemical potential. The latter case is presented in Figure 2. Indeed, thermal emissivities of both processes coincide for soft photons, and become different with increasing photon energy. Overall, our numerical results show a good agreement with the corresponding non-relativistic formulas.

In order to estimate accuracy of our calculations, we introduce the following quantity for each process

$$Q = n_{\mathrm{cut}}^{-1} \sum_a \left| \frac{\eta_a}{\eta_\gamma(e_a)} - 1 \right|, \tag{29}$$

where η_a is given by eq. (25) for Boltzmann statistics. This coefficient expresses the average relative deviation of numerical results from analytical ones for energy grid nodes. Limit of soft photons is adopted to summation index with upper boundary n_{cut} (namely $n_{\mathrm{cut}} = 15$ as $e_{15} = 0.01 = 0.1\theta$). Electron-electron bremsstrahlung emissivity is compared over full energy domain. Table II and Fig. 3 present values of Q for selected number of angular grid nodes. The relative error generally decreases with angular grid refinement. The Q value saturates for large number of nodes, which indicates that further energy grid refinement is needed. The relatively large errors for relativistic bremmstrahlung can be explained as follows. As calculations of Haug[63] show the differential cross section of bremsstrahlung strongly depends on angles even at nonrelativistic energies. Low resolution in angular grid does not allow to capture this strong dependence, which results in reduced accuracy, being compared to other interactions. Both energy and angular grid refinements provide substantial improvements of accuracy for bremsstahlung, see Fig. 5 and 6

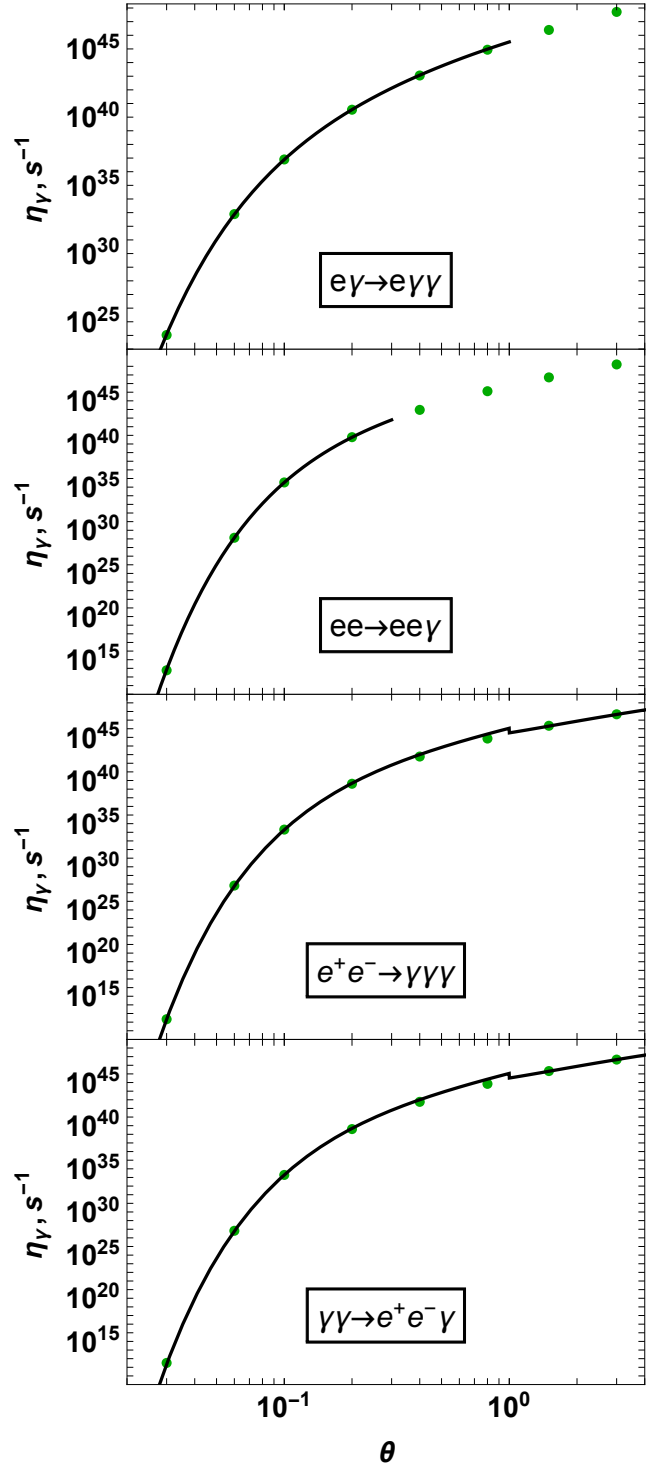below. Overall convergence of numerical results to the corresponding analytical ones is from good to satisfactory.

FIG. 4. Thermal photon emissivity η_γ as a function of temperature with fixed energy $e = 0.05 k_B T$. Solid curves represent Svennson[68] and Haug[24] analytical formulas, see text for details.

We also present the results of calculations in a wide temperature region $\theta = \{0.03, 0.06, 0.1, 0.2, 0.4, 0.8, 1.5, 3\}$ which
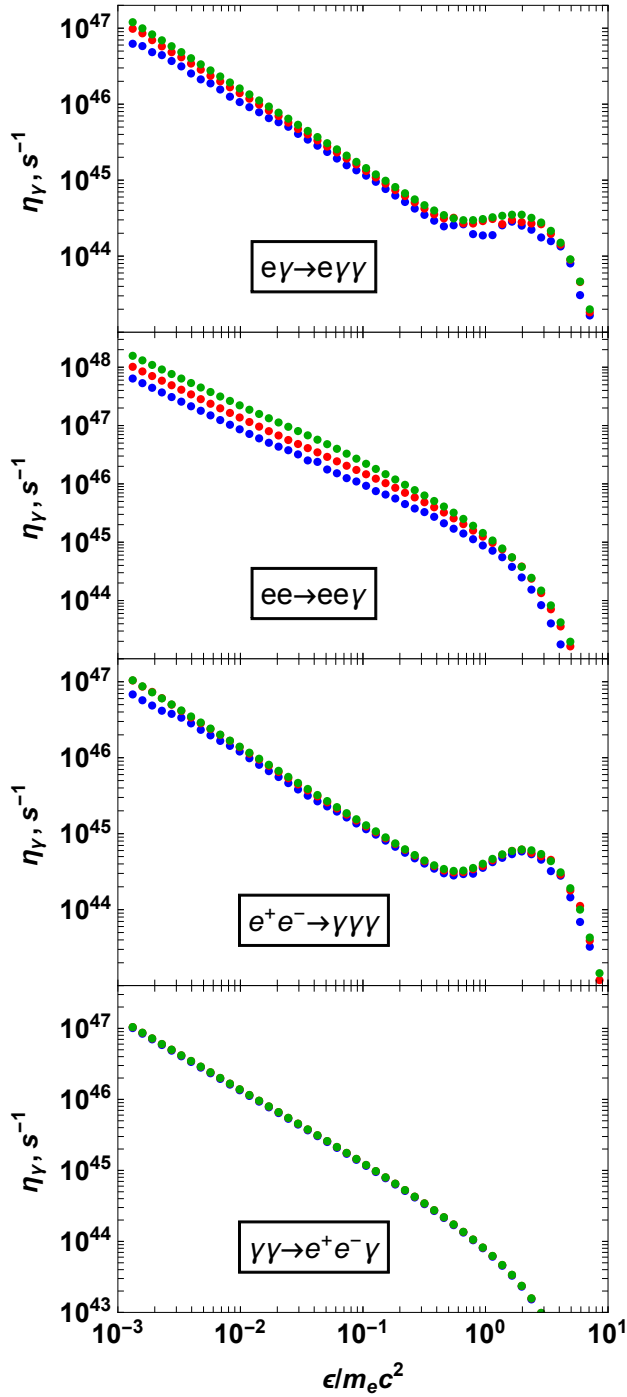
FIG. 5. Convergence of emission coefficients with increasing grid resolution, for a fixed temperature $\theta = 1$. The number of nodes in angles is 4 (blue dots), 8 (red dots), 16 (green dots), the number of energy nodes is 60. From top to bottom: double Compton scattering, relativistic bremsstrahlung, three-photon annihilation, radiative pair production.
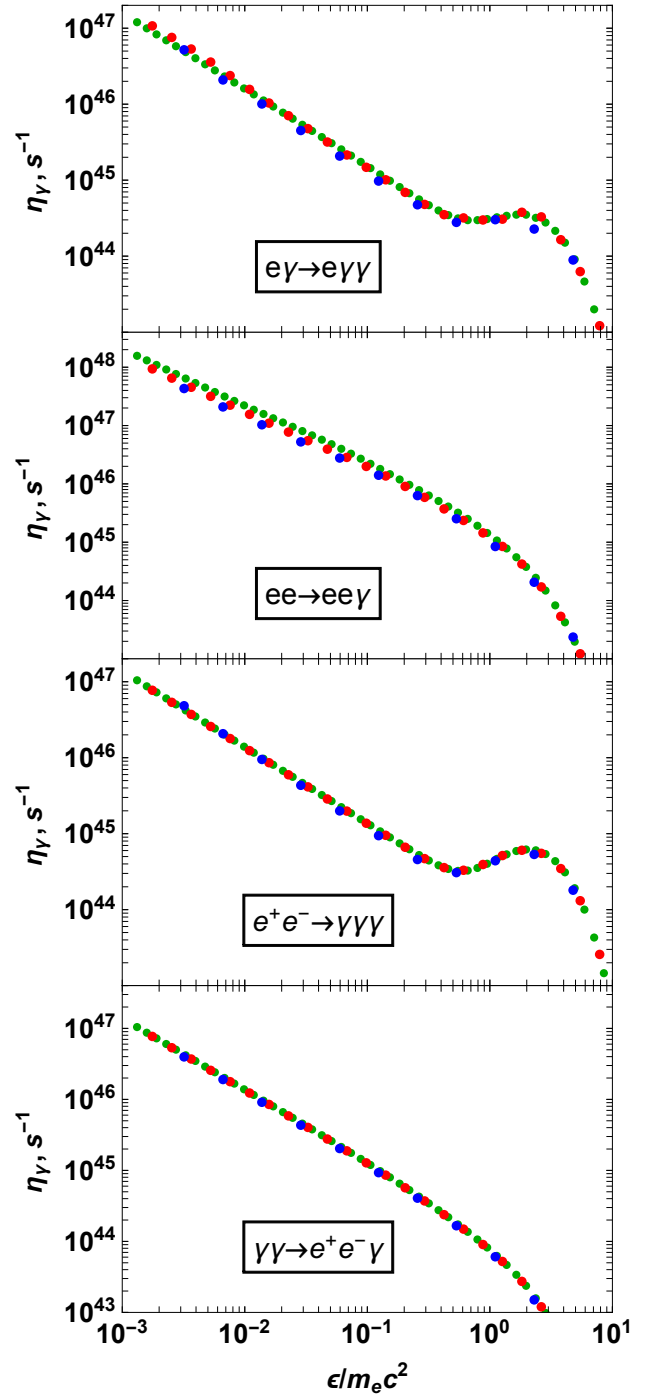
FIG. 6. Convergence of emission coefficients with increasing grid resolution, for a fixed temperature $\theta = 1$. The number of nodes in energy is 15 (blue dots), 30 (red dots), 60 (green dots), the number of nodes in angles is 16. From top to bottom: double Compton scattering, relativistic bremsstrahlung, three-photon annihilation, radiative pair production.

extends from non-relativistic to mildly relativistic temperatures. We provide a comparison with a fixed photon energy in the soft photon limit, here $e = 0.05\theta$. The result is shown in Figure 4, where black solid curve show analytic curves of Svensson and Haug. The analytical curve for double Compton scattering is plotted up to $\theta = 1$, and the non-relativistic analytical curve for bremsstrahlung is plotted up to $\theta = 0.3$. Three-photon annihilation and radiative pair production are compared with the same analytic curves (normalized to different number densities), which consist of two segments: non-relativistic one plotted up to $\theta = 1$ and relativistic one plotted above $\theta = 1$.

The convergence of our results is demonstrated in Figures 5 and 6, where we present the dependence of emission coefficients at fixed temperature $\theta = 1$ with varying number of nodes in angles (Fig. 5) and in energy (Fig. 6).

V. CONCLUSIONS

In this work we present the first principle calculations of collision integrals in triple interactions in relativistic plasma, including double Compton scattering, relativistic bremsstrahlung, radiative pair production and three photon creation/annihilation. These processes are important radiative processes in relativistic plasmas, and their account is essential also in the studies of non-equilibrium plasmas. The collision integrals are computed directly by numerical integration of vacuum QED matrix elements over the phase space of interacting particles on the finite grid. The plasma dressing effects such as Debye screening are not considered. Uehling-Uhlenbeck collision integrals computed in this scheme account for quantum statistics of particles, therefore strongly degenerate plasma can be modelled as well. The proposed method allows solution of relativistic kinetic equations for arbitrary non-equilibrium distribution functions, which take into account all triple interactions for the first time. This is an important new step, as most existing kinetic codes do not include triple interactions, and only few include them in a simplified way. In addition, our method can be applied to other processes for which matrix elements are known, such as neutrino interactions.

The comparison with existing analytic results for thermal distributions shows good agreement, with relative errors in the calculations not exceeding few percent, except for the case of relativistic bremsstrahlung where the error can reach up to 20 percent. The convergence of interaction rates with increasing grid resolution is demonstrated.

The new kinetic code, which computes binary and triple interactions in relativistic plasma out of first principles has wide applications in astrophysics, as well as for description of plasmas generated in laboratory.

ACKNOWLEDGMENTS

[1] A. G. Aksenov, R. Ruffini, and G. V. Vereshchagin, "Thermalization of Nonequilibrium Electron-Positron-Photon Plasmas," Phys. Rev. Lett. **99**, 125003–+ (2007), arXiv:0707.3250.

[2] R. Ruffini, G. Vereshchagin, and S.-S. Xue, "Electron-positron pairs in physics and astrophysics: From heavy nuclei to black holes," Physics Reports **487**, 1–140 (2010), arXiv:0910.0974 [astro-ph.HE].

[3] G. Vereshchagin and A. Aksenov, *Relativistic Kinetic Theory: With Applications in Astrophysics and Cosmology* (Cambridge University Press, 2017).

[4] A. Di Piazza, C. Müller, K. Z. Hatsagortsyan, and C. H. Keitel, "Extremely high-intensity laser interactions with fundamental quantum systems," Reviews of Modern Physics **84**, 1177–1228 (2012), arXiv:1111.3886 [hep-ph].

[5] T. A. Weaver, "Reaction rates in a relativistic plasma," Phys. Rev. A **13**, 1563–1569 (1976).

[6] R. J. Gould, "Kinetic theory of relativistic plasmas," Physics of Fluids **24**, 102–107 (1981).

[7] R. J. Gould, "Processes in relativistic plasmas," ApJ **254**, 755–766 (1982).

[8] S. Stepney, "Two-body relaxation in relativistic thermal plasmas," MNRAS **202**, 467–481 (1983).

[9] P. S. Coppi and R. D. Blandford, "Reaction rates and energy distributions for elementary processes in relativistic pair plasmas," MNRAS **245**, 453–507 (1990).

[10] C. D. Dermer, "Binary collision rates of relativistic thermal plasmas. I Theoretical framework," ApJ **295**, 28–37 (1985).

[11] R. Svensson, "Electron-Positron Pair Equilibria in Relativistic Plasmas," ApJ **258**, 335–+ (1982).

[12] A. A. Zdziarski, "Spectra from pair-equilibrium plasmas," ApJ **283**, 842–847 (1984).

[13] G. S. Bisnovatyi-Kogan, Y. B. Zel'Dovich, and R. A. Syunyaev, "Physical Processes in a Low-Density Relativistic Plasma." Soviet Ast. **15**, 17–+ (1971).

[14] A. P. Lightman, "Relativistic thermal plasmas - Pair processes and equilibria," ApJ **253**, 842–858 (1982).

[15] P. W. Guilbert and S. Stepney, "Pair production, Comptonization and dynamics in astrophysical plasmas," MNRAS **212**, 523–544 (1985).

[16] R. Svensson, "The pair annihilation process in relativistic plasmas," Astrophysical Journal **258**, 321–334 (1982).

[17] E. Haug, "Electron-positron bremsstrahlung in mildly relativistic thermal plasmas," A&A **148**, 386–390 (1985).

[18] E. Haug, "Energy loss and mean free path of electrons in a hot thermal plasma," A&A **191**, 181–185 (1988).

[19] A. P. Lightman, "Double Compton emission in radiation dominated thermal plasmas," ApJ **244**, 392–405 (1981).

[20] R. J. Gould, "The cross section for double Compton scattering," ApJ **285**, 275–278 (1984).

[21] J. W. Motz, H. A. Olsen, and H. W. Koch, "Pair Production by Photons," Reviews of Modern Physics **41**, 581–639 (1969).

[22] Y.-S. Tsai, "Pair production and bremsstrahlung of charged leptons," Reviews of Modern Physics **46**, 815–851 (1974).

[23] J. M. Jauch and F. Rohrlich, *The Theory of Photons and Electrons* (Springer-Verlag, 1976).

[24] E. Haug, "Electron-electron bremsstrahlung in a hot plasma." Zeitschrift Naturforschung Teil A **30**, 1546–1552 (1975).

[25] E. Haug, "Bremsstrahlung and pair production in the field of free electrons." Zeitschrift Naturforschung Teil A **30**, 1099–1113 (1975).

[26] M. S. Maxon and E. G. Corman, "Electron-Electron Bremsstrahlung from a Quantum Plasma (Z=1)," Physical Review **163**, 156–161 (1967).

[27] M. Alexanian, "Photon Bremsstrahlung from an Extreme-Relativistic Electron Gas," Physical Review **165**, 253–257 (1968).

[28] E. Haug, "Differential cross section of electron-positron bremsstrahlung," Phys. Rev. D **31**, 2120–2128 (1985).

[29] E. Haug, "On Energy and Angular Distributions of Electrons in Triplet Production," Zeitschrift Naturforschung Teil A **40**, 1182–1188 (1985).

[30] E. Haug, "Simple Analytic Expressions fot the Total Cross Section for γ-e Pair Production," Zeitschrift Naturforschung Teil A **36**, 413–414 (1981).

[31] A. Ore and J. L. Powell, "Three-Photon Annihilation of an Electron-Positron Pair," Physical Review **75**, 1963–1963 (1949).

[32] A. M. Frolov, "Three-photon annihilation of the electron positron pairs," Physics Letters A **372**, 6396–6399 (2008), arXiv:0809.1199 [hep-th].

[33] F. Mandl and T. H. R. Skyrme, "The Theory of the Double Compton Effect," Proceedings of the Royal Society of London Series A **215**, 497–507 (1952).

[34] R. J. Gould, "Soft-photon emission effects and radiative corrections for electromagnetic processes at very high energies." ApJ **230**, 967–973 (1979).

[35] J. Chluba, S. Y. Sazonov, and R. A. Sunyaev, "The double Compton emissivity in a mildly relativistic thermal plasma within the soft photon limit," A&A **468**, 785–795 (2007), arXiv:astro-ph/0611172 [astro-ph].

[36] A. P. Lightman and D. L. Band, "Relativistic thermal plasmas - Radiation mechanisms," ApJ **251**, 713–726 (1981).

[37] K. S. Thorne, "Relativistic radiative transfer - Moment formalisms," MN-RAS **194**, 439–473 (1981).

[38] J. Chluba, A. Ravenni, and S. K. Acharya, "Thermalization of large energy release in the early Universe," arXiv e-prints , arXiv:2005.11325 (2020), arXiv:2005.11325 [astro-ph.CO].

[39] G. Sarri, K. Poder, J. M. Cole, W. Schumaker, A. di Piazza, B. Reville, T. Dzelzainis, D. Doria, L. A. Gizzi, G. Grittani, S. Kar, C. H. Keitel, K. Krushelnick, S. Kuschel, S. P. D. Mangles, Z. Najmudin, N. Shukla, L. O. Silva, D. Symes, A. G. R. Thomas, M. Vargas, J. Vieira, and M. Zepf, "Generation of neutral and high-density electron-positron pair plasmas in the laboratory," Nature Communications **6**, 6747 (2015).

[40] R. Duclous, J. G. Kirk, and A. R. Bell, "Monte Carlo calculations of pair production in high-intensity laser-plasma interactions," Plasma Physics and Controlled Fusion **53**, 015009 (2011), arXiv:1010.4584 [hep-ph].

[41] T. Moritaka, L. Baiotti, A. Lin, L. Weiwu, Y. Sakawa, Y. Kuramitsu, T. Morita, and H. Takabe, "Plasma particle-in-cell simulations with QED reactions for pair production experiments using a high-Z solid target," in *Journal of Physics Conference Series*, Journal of Physics Conference Series, Vol. 454 (2013) p. 012016.

[42] C. Cercignani and G. Kremer, *The Relativistic Boltzmann Equation: Theory and Applications*, Progress in Mathematical Physics (Birkhäuser Basel, 2012).

[43] S. Groot, W. Leeuwen, and C. Weert, *Relativistic kinetic theory: principles and applications* (North-Holland Pub. Co., 1980).

[44] A. Pe'er and E. Waxman, "Time-dependent Numerical Model for the Emission of Radiation from Relativistic Plasma," Astrophysical Journal **628**, 857–866 (2005), astro-ph/0409539.

[45] M. A. Prakapenia, I. A. Siutsou, and G. V. Vereshchagin, "Numerical scheme for treatment of Uehling-Uhlenbeck equation for two-particle interactions in relativistic plasma," Journal of Computational Physics **373**, 533–544 (2018), arXiv:1801.02408 [astro-ph.HE].

[46] J. Chluba and R. A. Sunyaev, "The evolution of CMB spectral distortions in the early Universe," MNRAS **419**, 1294–1314 (2012), arXiv:1109.6552 [astro-ph.CO].

[47] A. G. Aksenov, M. Milgrom, and V. V. Usov, "Structure of Pair Winds from Compact Objects with Application to Emission from Hot Bare Strange Stars," ApJ **609**, 363–377 (2004), arXiv:astro-ph/0309014.

[48] A. G. Aksenov, R. Ruffini, and G. V. Vereshchagin, "Thermalization of pair plasma with proton loading," in *American Institute of Physics Conference Series*, American Institute of Physics Conference Series, Vol. 1111, edited by G. Giobbi, A. Tornambe, G. Raimondo, M. Limongi, L. A. Antonelli, N. Menci, and E. Brocato (2009) pp. 344–350.

[49] A. G. Aksenov, R. Ruffini, and G. V. Vereshchagin, "Thermalization of the mildly relativistic plasma," Phys. Rev. D **79**, 043008 (2009), arXiv:0901.4837 [astro-ph.HE].

[50] A. G. Aksenov, R. Ruffini, and G. V. Vereshchagin, "Kinetics of the mildly relativistic plasma and GRBs," in *American Institute of Physics Conference Series*, American Institute of Physics Conference Series, Vol. 1205, edited by R. Ruffini and G. Vereshchagin (2010) pp. 11–16.

[51] A. G. Aksenov, R. Ruffini, and G. V. Vereshchagin, "Pair plasma relaxation time scales," Phys. Rev. E **81**, 046401 (2010), arXiv:1003.5616 [astro-ph.HE].

[52] A. Benedetti, R. Ruffini, and G. Vereshchagin, "Phase space evolution of pairs created in strong electric fields," Physics Letters A **377**, 206 – 215 (2013).

[53] M. A. Prakapenia, I. A. Siutsou, and G. V. Vereshchagin, "Thermalization of electron-positron plasma with quantum degeneracy," Physics Letters A **383**, 306–310 (2019), arXiv:1810.10420 [astro-ph.HE].

[54] E. A. Uehling, "Transport Phenomena in Einstein-Bose and Fermi-Dirac Gases. II," Physical Review **46**, 917–929 (1934).

[55] E. A. Uehling and G. E. Uhlenbeck, "Transport Phenomena in Einstein-Bose and Fermi-Dirac Gases. I," Physical Review **43**, 552–561 (1933).

[56] M. A. Prakapenia and G. V. Vereshchagin, "Bose-Einstein condensation in relativistic plasma," (Europhysics Letters) **128**, arXiv:1908.04402 (2020), arXiv:1908.04402 [physics.plasm-ph].

[57] M. A. Prakapenia and G. V. Vereshchagin, "Pauli blocking effects in thermalization of relativistic plasma," Physics Letters A , arXiv:2003.07288 (2020), arXiv:2003.07288 [physics.plasm-ph].

[58] The quantum state is defined not only by momentum, but also by the spin projection. For isotropic distributions complete averaging over spins is performed, and quantum states are denoted by momentum implicitly summing over all possible spin states with the use of spin multiplier $g = 2s + 1$ for massive particles and $g = 2(1)$ for massless particles with spin $s > 0$ ($s = 0$). Therefore in this work plasma particles are assumed to be unpolarized.

[59] J. Chluba, *Spectral Distortions of the Cosmic Microwave Background*, Ph.D. thesis, Ludwig-Maximilians-Universität München (2005).

[60] V. B. Berestetskii, E. M. Lifshitz, and V. B. Pitaevskii, *Quantum Electrodynamics*, 2nd ed. (Elsevier, 1982).

[61] L. D. Landau and E. M. Lifshits, *The Classical Theory of Fields*, 4th ed. (Butterworth-Heinemann, 1994).

[62] J. M. Jauch and F. Rohrlich, *Texts and Monographs in Physics, New York: Springer, 1976, 2nd ed.* (Springer, New York, 1976).

[63] E. Haug and W. Nakel, *World Scientific Publishing Co., Singapore; ISBN 981-238-578-9* (World Scientific Publishing Co., Singapore, 2004).

[64] J. Ehlers, "Survey of general relativity theory," in *Relativity, Astrophysics and Cosmology* (1973) pp. 1–125.

[65] Alternatively, cylindrical coordinates can be used, if anisotropy is present in the problem, see e.g.[52].

[66] G. Hall and J. M. Watt, *Modern Numerical Methods for Ordinary Differential Equations* (New York, Oxford University Press, 1976).

[67] In order to satisfy exactly momentum conservation additional splitting is needed in angular grid[52].

[68] R. Svensson, "Steady mildly relativistic thermal plasmas - Processes and properties," MNRAS **209**, 175–208 (1984).